Real Space Measurement of Structure in Phase Separating Binary Fluid Mixtures

W. R. White* and Pierre Wiltzius
AT&T Bell Laboratories, 600 Mountain Avenue, Murray Hill, New Jersey 07974
(Received 29 June 1995)

In off-critical binary fluid mixtures undergoing phase separation, a polydisperse set of minority phase domains grows in a matrix of the majority phase. With confocal microscopy and digital image processing, we have made direct three-dimensional measurements of structure in phase separated mixtures of low molecular weight polymers. The distribution of domain sizes and the spatial correlations in these mixtures exhibit dynamic scaling, implying that the coarsening may be viewed entirely as an increase in length scale. This coarsening process appears to be driven by aggregation of domains.

PACS numbers: 83.70.Hq, 07.60.Pb, 61.43.Hv, 83.80.Es

Among the simplest forms of self-assembly is binary phase separation, in which two chemical components form a homogeneous mixture at high temperature, separating into two distinct phases upon cooling below a composition-dependent coexistence temperature $T_c(\Phi)$. If such a mixture is rapidly quenched from the single-phase region to a temperature below this coexistence curve, but above the spinodal decomposition curve $T_s(\Phi)$, then the mixture is metastable, and phase separation occurs by nucleation and growth of minority phase droplets inside a matrix of the majority phase [1]. If quenched below $T_s(\Phi)$, the mixture is unstable and rapidly separates into two spatially bicontinuous phases. In the latter case, the spatial structure is dominated by a single (maximally unstable) wavelength [2], and scattering techniques have been very effective in probing the dynamics of coarsening in this regime [3,4]. In the late stage of the nucleation and the growth regime, however, the minority phase droplets are quite polydisperse and can have complicated morphologies, preventing clear interpretation of scattering experiments. Attempts to study this regime [5] with conventional microscopy have been limited by the large depth of field of conventional microscopes, which is typically much larger than the distance between droplets. Thus, many questions remain about the spatial structure and coarsening dynamics of off-critical mixtures undergoing phase separation.

In this Letter, we show that confocal fluorescence microscopy [6] can be used to make three-dimensional, real space measurements of structure in phase separating off-critical mixtures. With this technique, we directly determine domain size distributions and spatial correlations at various coarsening times in polymer mixtures with low minority phase volume fractions ($2.1\% < \phi < 6.7\%$). While many previous studies have been made [7] of the real space structure in phase separating systems, these relied on inferring three-dimensional structural information from isolated two-dimensional sections. Also, many of these works examined metal alloy systems in which one phase was often a crystalline solid. In this case, the dynamics of domain coarsening may well be related to the dynamics of defects in the solid phase [8]. In our experiments, the domain size distributions observed are not consistent with those expected for coarsening by the evaporation-condensation mechanism, in which minority phase domains grow by molecular diffusion through the majority phase. Instead, coarsening appears to be driven primarily by coalescence of entire minority phase domains diffusing through the majority phase.

The mixtures studied consisted of low molecular weight (M_w), low polydispersity (M_w/M_n) oligomers of polystyrene ($M_w = 1475$, $M_w/M_n = 1.06$) and polybutadiene ($M_w = 2760$, $M_w/M_n = 1.08$), both obtained commercially [9]. A fluorescent dye, Pyrromethene 580 (0.005% by weight), was added to provide contrast between the phases. At the low molecular weights used here, the polymer chains are not long enough to permit significant entanglement, so that both materials should behave as simple fluids, although with very large viscosities [10]. All samples were prepared in solution with Tetrahydrofuran (THF), dried in a vacuum oven, and loaded into optical microscopy cells. One polybutadiene- (PB-) rich mixture and three polystyrene- (PS-) rich mixtures were studied. All of the PS-rich samples has the same composition, 75% PS by volume, but a different minority phase volume fraction ϕ was obtained in each sample by variation of the quench depth. After annealing for several hours in the one-phase region, samples were quenched into the nucleation and growth regime. In the PS-rich samples, the quench temperatures chosen were 61, 62.5, and 63.5 °C, producing $\phi = 6.7\%$, 4.0%, and 2.1%, respectively. The samples were allowed to coarsen for specified times (20 to 320 h) at the chosen quench temperature, and then frozen for imaging with a second quench to room temperature. With a commercial confocal microscope [11], operating in fluorescence mode with 514 nm illumination, we acquired several series of optical sections through each sample at each time. Each series contained 30–50 sections separated in depth by a distance of 0.3 μm, with lateral resolution of approximately 0.3 μm, allowing three-

 0031-9007/95/75(16)/3012(4)$06.00

dimensional imaging of micron-size features. To avoid surface effects, the uppermost section was acquired 5 μm below the sample surface. Figure 1 shows a typical fluorescence section in a PS-rich sample with $\phi = 2.1\%$ that has been allowed to coarsen for 160 h. In this image, regions of higher intensity represent cross sections through the nearly spherical PB-rich domains. At present, we do not know whether the fluorescence contrast between the phases arises primarily from concentration of the dye in the PB-rich phase or from partial quenching of the dye in the PS-rich phase. In the late stage of phase separation, the boundaries between phases are quite sharp, and the apparent width of the boundaries in Fig. 1 represents the resolution of the microscope. With computer image analysis, we "binarize" each optical section, assigning each pixel a value of 1 in the PS-rich matrix phase and 0 in the PB-rich droplets. Standard techniques [12,13] were employed for this purpose. Series of binarized sections were then recombined to form a three-dimensional binary array representing the domain structure of the sample. From this array, we determine the size and location of each of the minority phase domains, as well as the overall minority phase volume fraction of the sample.

In Fig. 2(a), we show $F(R,t)$, the distribution of domain radii R, at various coarsening times t, in a PS-rich sample with $\phi = 2.1\%$. While the domain sizes increase with time, the volume fraction remains constant, resulting in a monotonically decreasing density of minority phase domains. As a check of our image processing, we have verified that ϕ remains constant within 0.2% as a function of time. Similar results were obtained for PS-rich samples with $\phi = 4.0\%$ and 6.7%. From these size distribution functions, we calculate the time dependence of the average domain radius $\overline{R}(t)$ at each volume fraction, shown in Fig. 3(a). In each case, the growth of the mean domain size is well described by a power law, $\overline{R}(t) = k(\phi)t^{1/3} + \overline{R}(0)$. In Fig. 2(b), we show the radial distribution function (the normalized pair correlation function) of droplet centers, $G(x,t)$, measured at various times in the $\phi = 2.1\%$ sample. As seen here the density of droplets is suppressed in the immediate vicinity of a given droplet, and the size of this depletion zone increases as the droplets coarsen.

If at each coarsening time we rescale all lengths by the average domain size at that time, we see that both the size distribution functions and the radial distribution functions exhibit dynamic scaling. Specifically, if we examine the size distributions in Fig. 2(a), dividing the horizontal axis by $\overline{R}(t)$, and multiplying the vertical axis by $\alpha\overline{R}^4(t)$, we see that each of the curves collapses onto a single, time independent, scaled size distribution function $f(R/\overline{R},\phi)$, as shown in Fig. 2(c). The normalization constant α is chosen to make the integrated area under the scaled curve equal to unity at $t = 20$ h. The radial distribution functions may also be collapsed onto a single scaled radial distribution function $g(x/\overline{R},t)$, shown in Fig. 2(d). In this case, we need only divide the horizontal axis by $\overline{R}(t)$, since $G(x,t)$ is dimensionless. Thus the distribution functions can be written in the scaling forms $F(R,t) = f(R/\overline{R},\phi)/\alpha\overline{R}^4(t)$ and $G(x,t) = g(x/\overline{R},\phi)$. Physically this signifies that the coarsening may be viewed entirely as an increase of length scale, without any change in basic

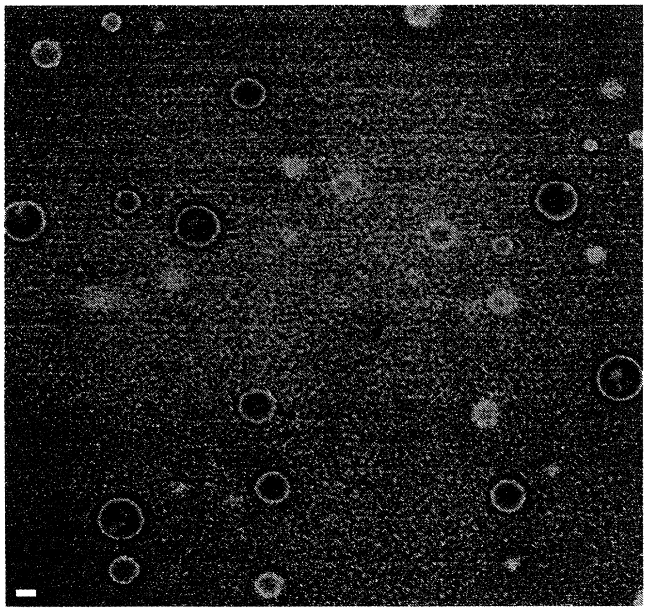

FIG. 1(color). False color image of fluorescence intensity in a section at depth $d = 8.0$ μm below the surface of a PS-rich sample with volume fraction $\phi = 2.1\%$. Bright regions represent sections through nearly spherical PB-rich domains. The apparent boundary width arises from the finite lateral and depth resolution 0.3 and 0.7 μm, respectively. The scale bar is 1.0 μm.

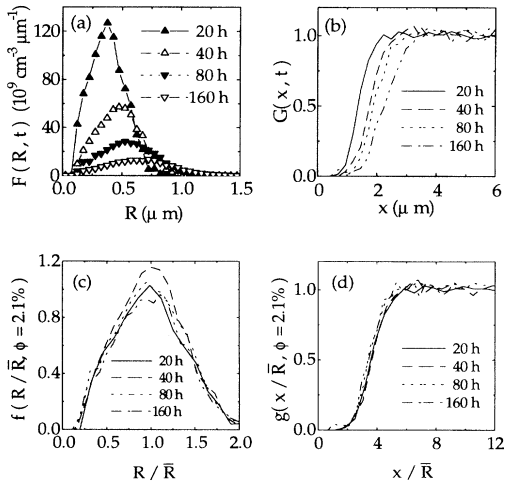

FIG. 2. Structural properties measured at various coarsening times in a PS-rich sample with $\phi = 2.1\%$. (a) Domain size distributions. (b) Radial distribution functions. (c) Scaled domain size distributions. (d) Scaled radial distribution functions. The scaled distribution functions shown in (c) and (d) are derived by scaling all lengths in the measured distribution functions at a given time by the mean domain size at that time.

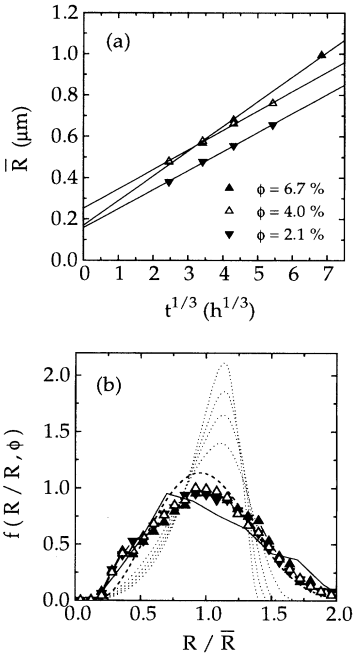

FIG. 3. Volume fraction dependence of structure observed in PS-rich samples. (a) Time dependence of average domain radii. (b) Comparison of measured scaled domain size distributions with those expected from coarsening by various models. Solid lines: measured size distributions in PS-rich samples (with points) and in the PB-rich sample (without points). The points associated with various volume fractions are as shown in the legend of (a). Dashed lines: size distributions expected from Smoluchowski aggregation of perfectly sticking spheres (heavy dashes) and evaporation or condensation at $\phi = 0\%$, 1%, 3%, and 6% (multiple dotted lines, peak height decreases with increasing ϕ). The aggregation result was obtained by numerical integration of the Smoluchowski rate equations, and the evaporation-condensation result was taken from Ref. [15].

structure. In the scaled distributions, we explicitly include the variable ϕ to denote the possibility that the scaled functions could depend on volume fraction. In fact, $f(R/\overline{R}, \phi)$ shows no discernible dependence on ϕ, as demonstrated in Fig. 3(b). The scaled radial distributions, however, do depend on ϕ, developing [13] a small peak with increasing ϕ. This peak arises from packing constraints and corresponds to the development of a weakly preferred interdroplet spacing at higher volume fractions.

What can we learn from these structural observations about the mechanism of domain coarsening? In the evaporation-condensation picture, the exact results [14] of Lifshitz and Slyozov (valid as $\phi \to 0$) and numerical simulations [15,16] at finite volume fraction predict that the average domain size increases as $\overline{R}(t) = k_e(\phi)t^{1/3} + \overline{R}(0)$, in agreement with our observations. The predicted ϕ dependence of the coarsening rate constant $k_e(\phi)$ decreases as ϕ decreases but approaches a nonzero value as $\phi \to 0$. While this power law growth agrees with that seen in experiment, a similar growth law would be expected from coalscence of droplets colliding while undergoing diffusive Brownian motion [17]. A mean field description of such a process would be given by the aggregation rate equations [18] of Smoluchowski, coupled with the Stokes-Einstein relation for the diffusivity of spherical domains moving through a viscous matrix. In this model, the mean domain size is also known [18] to grow as $\overline{R}(t) = k_c(\phi)t^{1/3} + \overline{R}(0)$. Here the growth rate constant is expected to have the form $k_c(\phi) \propto \phi^{1/3}$, in contrast to the evaporation-condensation model, in which $k_e(\phi)$ approaches a nonzero value as $\phi \to 0$. In principle then, the measured rate constants $k(0)$ should be useful in determining the primary growth mechanism, since growth rates in the two models behave quite differently as $\phi \to 0$. In practice, the rate constants in both models have such a weak ϕ dependence in the range measured that we cannot differentiate on this basis without more accurate measurements of domain sizes or measurements at much lower values of ϕ. If we examine the scaled size distributions, however, we see a clear distinction between the models. In the evaporation-condensation picture, $f(R/\overline{R}, \phi)$ should [15] be sharply peaked and highly asymmetric as $\phi \to 0$, becoming increasingly broad and symmetric with increasing ϕ, as shown in Fig. 3(b). In the range of volume fractions studied here, a substantial ϕ dependence of $f(R/\overline{R}, \phi)$ is expected in this model, and none is observed experimentally. This model also predicts size distributions more narrow than those observed. In the Smoluchowski model of coalescence, however, the scaled size distributions are expected to be ϕ independent and are in good agreement with the observed size distributions, as seen in Fig. 3(b).

If we now examine the PB-rich mixture, we see clear evidence of domain growth by coalescence. In Fig. 4, we show a section through the PB-rich sample ($\phi = 7.9\%$, coarsened 20 h), directly demonstrating that the PS-rich minority phase domains are formed by aggregation of smaller demains. The PS-rich domains appear dark in Fig. 4. Although the domains are not spherical, we may compare the domain size distribution in this sample with that in the PS-rich samples by measuring the volume V_i of each domain and assigning an effective radius $R_i = [(3/4\pi)/V_i]^{1/3}$. As shown in Fig. 3(b), the scaled distribution of effective radii in the PB-rich sample is very nearly the same as the scaled distribution of radii in the PS-rich samples, indicating that the scaled distributions of domain volumes are the same in both cases, although the domain morphology is quite different. Thus it seems likely that the same mechanism drives coarsening on both sides of the coexistence curve.

If domains grow by aggregation on both sides of the coexistence curve, how can we understand the different morphologies in the PS-rich and PB-rich mixtures? This difference likely arises from the composition dependence of two time scales: t_c, the mean time between coalescence events for a given domain and t_r, the time required for the shape of an aggregate domain to relax

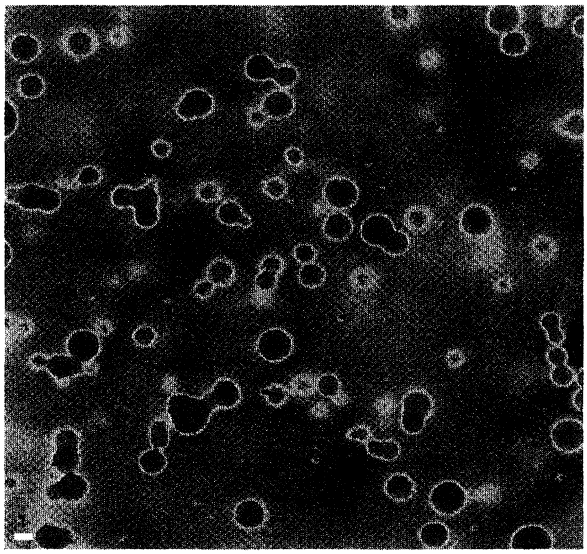

FIG. 4(color). Fluorescence intensity in a section 8.0 μm below the surface of the PB-rich sample. The PS-rich domains (dark regions) are clearly formed by aggregation.

to a sphere after coalescence. These times may be estimated [17] as $t_c \sim (\overline{R}\phi^{-1/3})^2/D \approx 6\pi\eta_m\overline{R}^3/kT\phi^{2/3}$ and $t_r \sim \eta_d\overline{R}/\sigma$, where D is the Stokes-Einstein diffusivity of the minority phase domains, η_d is the viscosity of the minority phase domains, η_m is the viscosity of the majority phase, and σ is the surface tension between phases. At early times (small values of $\overline{R}$), $t_c < t_r$, and the morphology should be of the type seen in Fig. 4. As $\overline{R}$ increases with t, the morphological relaxation will become rapid compared to the time between coalescence events, so that the domains should begin to assume a spherical morphology when the domains become larger than some crossover size $R_m = (\eta_d kT\phi^{2/3}/6\pi\eta_m\sigma)^{1/2}$. Since the viscosity of the polystyrene, η_{PS}, is much greater than the viscosity of the polybutadiene, η_{PB}, this crossover size will be dependent on composition. In the PS-rich samples, where $\eta_m \gg \eta_d$, the size at which the domains will become spherical is much smaller than in the PB-rich case, where $\eta_m \ll \eta_d$. To estimate the order of magnitude of R_m in the PS-rich samples, we begin by assuming that the viscosity of the PB-rich domains in the PS-rich samples is roughly the same as the viscosity of the PB-rich matrix in the PB-rich sample. The ratio η_m/η_d may then be estimated from the ratio of the growth rate constants in the PS-rich and PB-rich mixtures. Since the growth rate constant is roughly three times larger in the PB-rich mixture than in the PS-rich mixtures, we may very crudely estimate [17] $\eta_m/\eta_d \sim 25$ in the PS-rich samples. If we estimate σ from the Joanny-Leibler [19] result, we expect that $R_m \sim 0.05$ μm in the PS-rich samples. Since this crossover size is well below the resolution of our microscope, the domains in the PS-rich samples should always appear spherical in our experiments. Indeed, this crossover size may even be less than the size of the critical nucleus. If we perform a similar calculation for the PB-rich sample, we expect that $R_m \sim 1.0$ μm. Thus we would expect that, in this mixture, domains in the few micron size range will show the morphology observed in Fig. 4: clearly aggregated, but with substantial relaxation back to spheres.

In conclusion, we have used confocal scanning fluorescence microscopy and quantitative image analysis to make direct measurements of domain size distributions and spatial correlations in phase separating binary fluid mixtures. To our knowledge, this work is the first direct measurement of these quantities in any three-dimensional system undergoing a first-order phase transition. In mixture of low molecular weight polymers with moderately low volume fractions, coarsening appear to occur almost entirely by domain coalescence. However, in mixtures with much lower volume fractions or much lower molecular weights than those studied here, the significance of the evaporation-condensation mechanism is still not established.

*Electronic address: white@physics.att.com

[1] J. Frenkel, *Kinetic Theory of Liquids* (Dover, New York, 1946).
[2] J. W. Cahn, Trans. Metall. Soc. AIME **242**, 166 (1968).
[3] W. I. Goldburg, in *Light Scattering Near Phase Transitions,* edited by H. Z. Cummins and P. Levanyuk (North-Holland, Amsterdam, 1983).
[4] F. S. Bates and P. Wiltzius, J. Chem. Phys. **91**, 3258 (1989).
[5] S. Krishnamurthy and W. I. Goldburg, Phys. Rev. A **22**, 2147 (1980).
[6] See *Confocal Microscopy,* edited by T. Wilson (Academic Press, London, 1990).
[7] S. C. Hardy and P. W. Voorhees, Metall. Trans. **19A**, 2713 (1988).
[8] W. A. Kaysser, S. Takajo, and G. Petzow, Acta Metall. **32**, 115 (1984).
[9] Pressure Chemical Co. and Polysciences, Inc.
[10] William W. Graessley, in *Physical Properties of Polymers* (American Chemical Society, Washington, D.C., 1984).
[11] Molecular Dynamics Multiprobe 2001, with inverted Nikon Diaphot microscope and 1.4 numerical aperture 100× oil immersion lens.
[12] Nicole Y. Morgan and M. Seul, J. Phys. Chem. **99**, 2088 (1995).
[13] W. R. White and Pierre Wiltzius (to be published).
[14] I. M. Lifshitz and V. V. Slyozov, J. Phys. Chem. Solids **19**, 35 (1961).
[15] Jian Hua Yao, K. R. Elder, Hong Guo, and Martin Grant, Phys. Rev. B **47**, 14 110 (1993).
[16] Norio Akaiwa and P. W. Voorhees, Phys. Rev. E **49**, 3860 (1994).
[17] Eric D. Siggia, Phys. Rev. A **20**, 595 (1979).
[18] Tamas Vicsek, *Fractal Growth Phenomena* (World Scientific, Singapore, 1989).
[19] J. F. Joanny and L. Leibler, J. Phys. (Paris) **39**, 951 (1978).

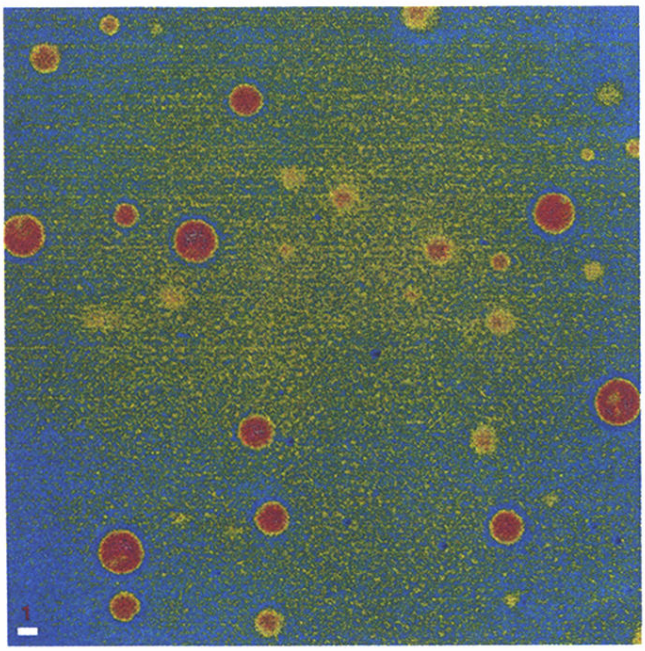

FIG. 1(color). False color image of fluorescence intensity in a section at depth $d = 8.0\ \mu$m below the surface of a PS-rich sample with volume fraction $\phi = 2.1\%$. Bright regions represent sections through nearly spherical PB-rich domains. The apparent boundary width arises from the finite lateral and depth resolution 0.3 and 0.7 μm, respectively. The scale bar is 1.0 μm.

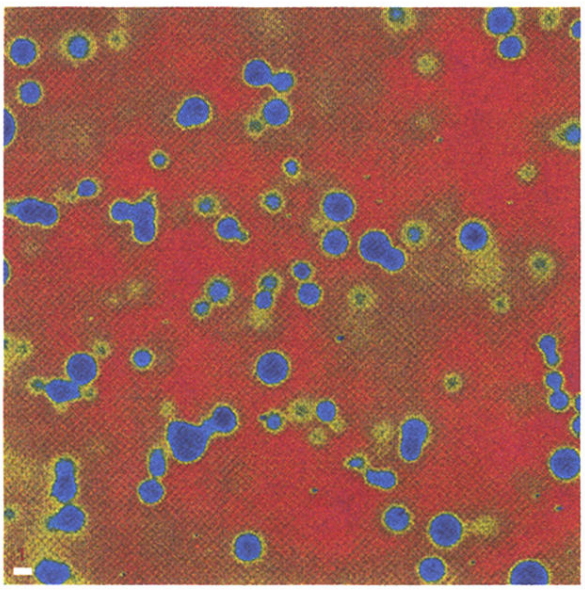

FIG. 4(color). Fluorescence intensity in a section 8.0 μm below the surface of the PB-rich sample. The PS-rich domains (dark regions) are clearly formed by aggregation.